Honeycomb, square, and kagomé vortex lattices in superconducting systems with multi-scale inter-vortex interactions

Qingyou Meng,[1] Christopher N. Varney,[2] Hans Fangohr,[3] and Egor Babaev[4,1]

[1]*Department of Physics, University of Massachusetts, Amherst, Massachusetts 01003, USA*
[2]*Department of Physics, University of West Florida, Pensacola, FL 32514, USA*
[3]*Engineering and the Environment, University of Southampton SO17 1BJ, UK*
[4]*Department of Theoretical Physics, The Royal Institute of Technology, SE-10691 Stockholm, Sweden*

The recent proposal of Romero-Isart *et al.* [1] to utilize the vortex lattice phases of superconducting materials to prepare a lattice for ultra-cold atoms-based quantum emulators, raises the need to create and control vortex lattices of different symmetries. Here we propose a mechanism by which honeycomb, hexagonal, square, and kagomé vortex lattices could be created in superconducting systems with multi-scale inter-vortex interaction. Multiple scales of the inter-vortex interaction can be created and controlled in layered systems made of different superconducting material or with differing interlayer spacing.

PACS numbers: 67.85.-d, 74.25.Uv,

To circumvent the limitations on classical computation, a growing effort to manipulate and control the behavior of ultracold atomic gases has led to these systems being used as quantum simulators for a host of phenomena in condensed matter physics [2, 3]. A focus of quantum simulator investigations has been on building Hubbard models by loading a gas of neutral atoms into optical lattices and tuning the interaction between the atoms [4, 5]. At present, great strides have been made in cooling protocols [6–8]. But the main question, to assess in such experiments whether the Hubbard model can explain high-T_c superconductivity, remains unanswered.

In order to address this question, better cooling schemes which reduce the entropy of the quantum simulator are necessary [5]. Very recently, Romero-Isart *et al.* [1] proposed placing ultracold atoms in a lattice potential generated by magnetic field of superconducting vortices in type-2 superconductors and trapping the atoms near the surface. This new approach aims to decrease the inter-lattice site distance, making the required regimes experimentally feasible [1, 9]. This possibility of a crucially important application raises the need to create and control vortex lattices of different symmetries. Although in some exotic cases a square vortex lattice has been observed [10, 11], the overwhelming majority of vortex lattices in superconductors have hexagonal symmetry. In order to create a vortex lattice of various symmetries for quantum emulators, Romero-Isart *et al.* [1] proposed pinning the vortices in arrays of etched holes/anti-dots [12]. While such vortex systems have been extensively investigated in superconductivity both theoretically and experimentally for various pinning array geometries [13–22], Romero *et al.* [1] note that the anticipated challenges to implementing the approach are high requirements for perfection of the vortex lattice and possible variations and field inhomogeneities in the anti-dot arrays. In fact, the interest in self-assembly of kagomé and honeycomb structures goes beyond the recent interest in vortex matter and is intensively studied in soft condensed matter systems [23–26].

Here we propose an alternative approach involving multi-component superconducting systems. Recently there has been interest in superconductivity with several scales of repulsive and attractive interaction. In two-band superconductors it is possible to have a vortex system where the short-range interactions are repulsive while the long-range interactions are attractive in regimes where one coherence length is shorter than the magnetic field penetration length while the second coherence length is larger, i.e. $\xi_1 < \lambda < \xi_2$ [27–30]. The regime which was recently termed type-1.5 superconductivity in experimental works on MgB_2 [31–33] and Sr_2RuO_4 [34, 35]. The non-monotonic inter-vortex interaction is also possible in electromagnetically or proximity-effect coupled bilayers [27].

In the two-band superconductor the long-range inter-vortex interaction energy is given by [27, 28, 36]

$$E_{\text{int}} = C_B^2 K_0\left(\frac{r}{\lambda}\right) - C_1^2 2\pi K_0\left(\frac{r}{\xi_1}\right) - C_2^2 K_0\left(\frac{r}{\xi_2}\right). \tag{1}$$

The first term describes inter-vortex repulsion which comes from magnetic and current-current interaction. The second and third terms describes attractive interactions from cores overlaps. The two contributions are due to to coherence lengths.

In Ref. 37 it was proposed that in layered systems multiple repulsive length scales are possible when different layers have different λ_i. For a straight and rigid vortex line, the long-range interaction is then

$$E_{\text{int}} = \sum_i {C_B}_i^2 K_0\left(\frac{r}{\lambda_i}\right) - \sum_j C_j^2 2\pi K_0\left(\frac{r}{\xi_j}\right). \tag{2}$$

Such a system can have various cluster phases due to multi-scale repulsive interactions [37]. Subsequently

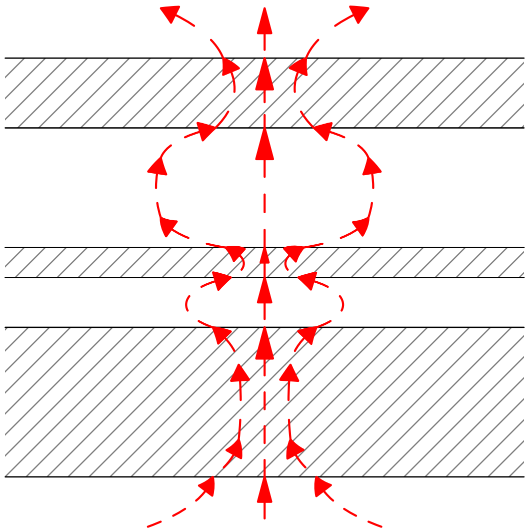

FIG. 1. Schematic picture of the magnetic field lines of a vortex in a layered superconductor. Shaded (white) areas are superconductor (insulator) layers with different thickness. The flux spreads in the non-superconducting regions.

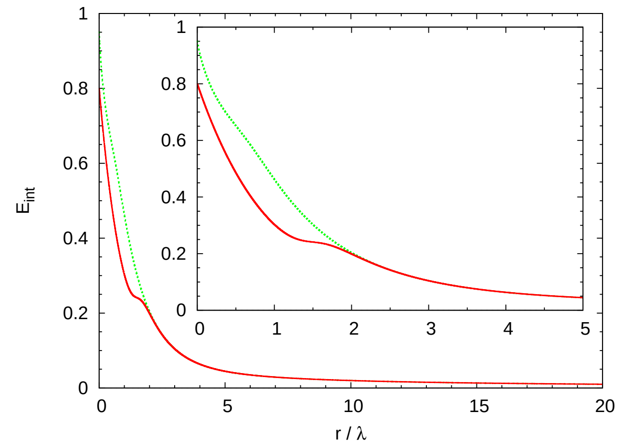

FIG. 2. Phenomenological potential that describes the multi-scale inter-vortex interaction for straight rigid vortex lines in layered system with different layer's parameters. The solid red curve gives rise to a honeycomb lattice at density [46] $\rho = 1.50$, a hexagonal lattice at $\rho = 2.25$, and a square lattice at $\rho = 2.50$, while for the dashed green line a kagomé lattice is the ground state at a density of $\rho = 2.50$. [47].

some of the phases obtained in simulations where the vortices are treated as a point-particle [37] were also obtained in simulations of a layered Ginzburg-Landau model [38].

Here we point out that layered systems proposed in Ref. 37, i.e. structures made of a combination of type-1 and type-2 superconductors with variable interlayer distances (see Fig. 1), could be used to create vortex lattice of different symmetries. In what follows, we utilize Langevin dynamics to study various states of vortex matter in superconductors [39–42]. Often in systems with multiple repulsive length scales various phases are quite robust with respect to potential changes as long as the potential preserves the distinct repulsive length scales [43, 44]. Thus we use a phenomenological pairwise potential with multiple length scales which has characteristic features of the analytically known asymptotic form Eq. (2) as well as included effect of demagnetization field in the form of analytically known long-range power-law repulsive inter-vortex force [45]. We demonstrate that layered systems where such a potential can be realized can be used to generate the four two-dimensional lattices: hexagonal, honeycomb, square, and kagomé.

In Fig. 2, we illustrate two potentials that arise from a phenomenological form

$$E_{\rm int} = c_1 e^{-r/\lambda} - c_2 e^{-r/\xi} + c_3 \frac{\lambda\{\tanh[\alpha(r-\beta)]+1\}}{r+\delta} \tag{3}$$

that captures the essential multi-scale features of the inter-vortex forces in a layered superconducting structure [37, 47], when the interaction can be approximated by pairwise forces between straight vortex lines. The model features a short-range exponential repulsion, intermediate-ranged exponential attraction, and a long-range power-law repulsive behavior. The interplay between these different interactions results in a rich phase diagram which go beyond the scope of this paper; we defer a full discussion of its properties for future work [48].

In Fig. 3, we illustrate some of the ground state vortex phases of the potentials shown in Fig. 2. The phases were obtained using Langevin dynamics [40] simulations of $N_v \approx 1000$ to $N_v \approx 3000$ vortices where the temperature was slowly reduced to $T = 0$ (see Refs. 37 and 48 for additional details). For the solid red line of Fig. 2, we obtain honeycomb, hexagonal, and square lattices at densities [46] $\rho = 1.50$, 2.25, and 2.50, respectively. For the dashed green curve, we obtain a perfect kagomé lattice for $\rho = 2.50$. For the honeycomb, hexagonal and square lattice results, we find little to no defects for the largest system sizes studied. For the kagomé lattice results, we achieve a defect-free lattice for 1020 vortices but observe a kagomé lattice with defects for 2958 vortices which may be a consequence of the simulated annealing rate. All simulations were initialized with random configurations and later compared with a perfect lattice. In the case of the honeycomb and kagomé lattice results, we observed a polycrystalline state which had higher energy than the perfect lattice. To ensure that the perfect lattice was the correct ground state, we prepared simualtions with the ground state configuration at high temperature repeated the simulated annealing protocol, ending up with a final configuration lower than the defect-filled case (see Fig. 3(a,d) for lowest energy configurations).

In order to characterize the degree of perfection for each phase, we first consider the radial distribution func-

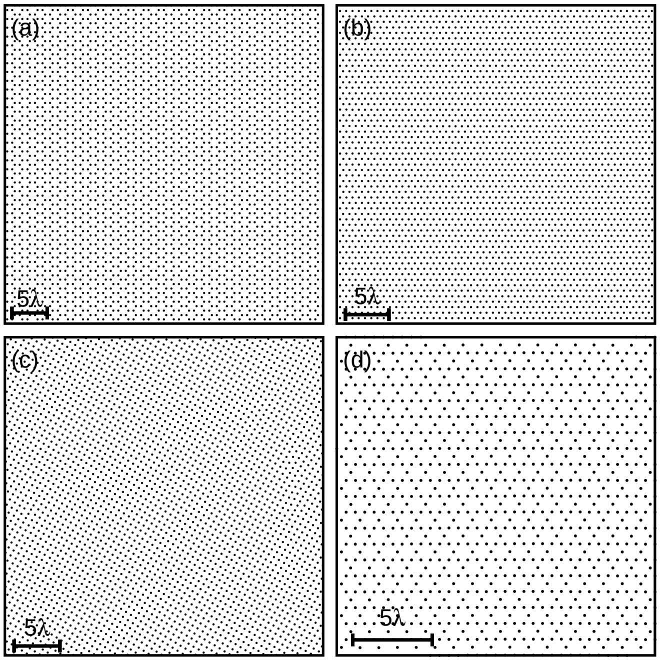

FIG. 3. The final vortex configuration at the zero temperature for (a) $N_v = 3024$ and $\rho = 1.50$ (honeycomb lattice), (b) $N_v = 2958$ and $\rho = 2.25$ (hexagonal lattice), (c) $N_v = 2958$ and $\rho = 2.50$ (square lattice), and (d) $N_v = 1020$ and $\rho = 2.50$ (kagomé lattice). Panels (a)-(c) correspond to the solid red curve of Fig. 2, while panel (d) corresponds to the dashed green curve.

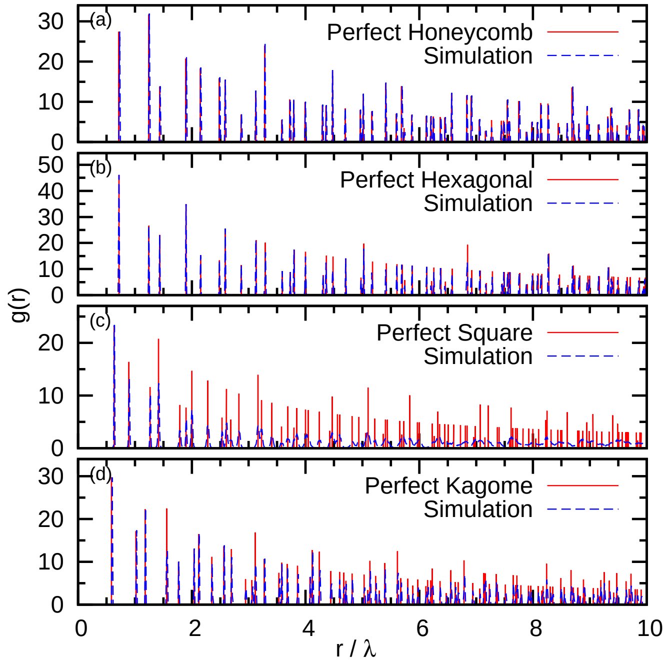

FIG. 4. Comparison of the radial distribution function $g(r)$ of the vortex configurations shown in Fig. 3 with those of the ideal geometry for (a) honeycomb, (b) hexagonal, (c) square, and (d) kagomé lattices. The dashed blue line is the zero temperature result after simulated annealing, and the solid red line is the ideal result.

tion (RDF),

$$g(r) = \frac{1}{2\pi r \Delta r \rho N_v} \sum_{i=1}^{N_v} n_i(r, \Delta r), \quad (4)$$

where $n_i(r, \Delta r)$ is the number of particles in the shell surrounding the i-th particle with radius r and thickness Δr. For phases that form regular lattice structures, we can offer a direct comparison with an ideal lattice, which we illustrate in Fig. 4.

From $g(r)$ we can define the i-th nearest neighbor (coordination numbers) as

$$n_i = 2\pi\rho \int_{r_{i-1}}^{r_i} g(r) dr, \quad (5)$$

where r_{i-1} and r_i are the minima surrounding the ith peak in $g(r)$. In Fig. 5, we show the coordination number up to the 5th nearest neighbor for each of the lattices shown above.

Next, we define the degree of perfection $d = \frac{1}{N_v}\sum d_j$ for a lattice as

$$d_j = \frac{1}{n_1} \left| \sum_{i=1}^{n_1} \left(1 - \frac{\Delta\theta}{\theta_{\text{perfect}}} \right) \right|, \quad \Delta\theta = |\theta_i - \theta_{\text{perfect}}| \quad (6)$$

where d_j is the degree of perfection for the jth vortex, n_1 is the number of the nearest neighbors (i.e. the number of the vortices within a circle of radius r_c with the jth vortex at its center, where r_c is the first minimum of the RDF), θ_i is the angle between the two nearest neighbours, and θ_{perfect} is the angle between the two nearest neighbours in the perfect lattice. Note that by definition, $d = 1$ if there are no defects in the lattice. For the square, hexagonal, and honeycomb lattices $\theta_{\text{perfect}} = \pi/2$, $\pi/3$, and $2\pi/3$, respectively, while the kagomé lattice has two possible angles: $\pi/3$ and $2\pi/3$.

For the honeycomb lattice (panel (a) of Figs. 3, 4, and 5), we find that the ordering of the vortices matches the ideal result very well, with the degree of perfection $d \approx 1$ for all simulations of $N_v = 1008$ and $N_v = 3024$ vortices. The peaks of the radial distribution function closely match the ideal case, with broadening of the peaks due to defects that increases as the separation between the vortices increases. The coordination number is within 1% for all results.

For the hexagonal lattice [panel (b)], the ordering is nearly perfect, with $d \approx 1$ and the radial distribution function featuring nearly delta function peaks that match with the ideal result. The coordination number calculation also remains within 1% of the ideal result up to n_5 for simulations of $N_v = 2958$ and for all coordination

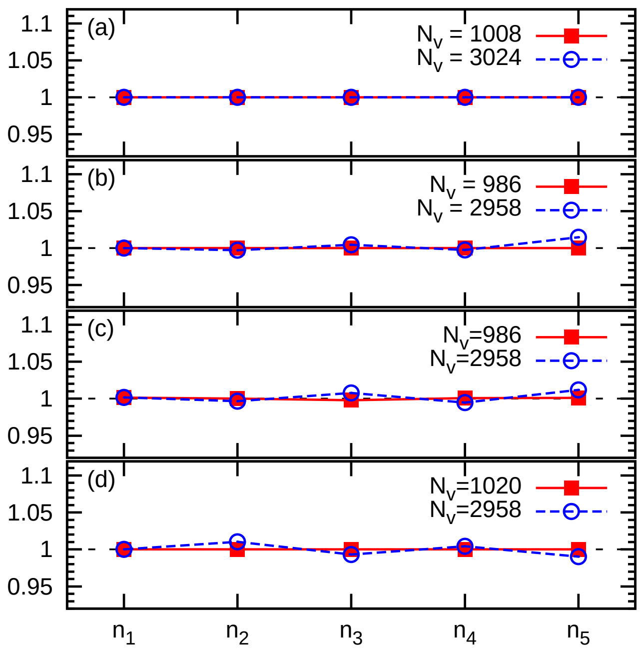

FIG. 5. Number of nearest neighbors n_i up to the fifth-nearest-neighbor for the (a) honeycomb (b) hexagonal, (c) square, and (d) kagomé lattices of Fig. 3 with $N_v \approx 1000$ (squares) and 3000 (circles) vortices. Here, n_i is normalized to the number of neighbors in a perfect lattice.

numbers we calculated for simulations of $N_v = 986$ vortices.

For the square lattice [panel (c)], the ordering is extremely good, with $d = 0.990$ and 0.989 for $N_v = 986$ and 2958 vortices, respectively. The radial distribution function features delta function peaks for the first eight peaks before broadening begins to occur. In addition, the number of nearest neighbors calculated is within 1% of the ideal result for the first five neighbors.

For the kagomé lattice [panel (d)], the ordering is also very good, with $d = 0.999$ and 0.946 for $N_v = 1020$ and 2958, respectively. The radial distribution function of the simulation result matches the perfect kagomé lattice peaks very well. The coordination numbers are within 1% for both $N_v = 1020$ and 2958 vortices.

In summary, the recent proposal [1] of realizing quantum emulators by trapping ultra-cold atoms in the magnetic field of superconducting vortex lattice raises the need to develop methods to create vortex lattices of various symmetries. Here we propose layered systems where vortex interaction is multi-scale (in particular the type-1.5 systems) as the systems where in principle various vortex lattice symmetries can be realized. The upper layer may in particular be used to tune localization of the field while lower layers and interlayer distances are used to control lattice symmetry. Different temperature dependencies of components in different layers can also be used to manipulate the vortex lattice by controlling the temperature. We support that proposal by simulation of point-particle objects with phenomenological two-body forces similar to long-range forces between straight and rigid vortex lines. Next we plan to investigate it in the layered Ginzburg-Landau model which also include the effects of vortex bending and non-pairwise inter-vortex forces (which can be especially important in type-1.5 regime [36]).

This work was supported by the National Science Foundation under the CAREER Award DMR-0955902, Knut and Alice Wallenberg Foundation through a Royal Swedish Academy of Sciences Fellowship, and by the Swedish Research Council.

[1] O. Romero-Isart, C. Navau, A. Sanchez, P. Zoller, and J. I. Cirac, Phys. Rev. Lett. **111**, 145304 (Oct. 2013)
[2] I. Buluta and F. Nori, Science **326**, 108 (Oct. 2009)
[3] J. I. Cirac and P. Zoller, Nature Phys. **8**, 264 (Apr. 2012)
[4] I. Bloch, J. Dalibard, and W. Zwerger, Rev. Mod. Phys. **80**, 885 (Jul. 2008)
[5] I. Bloch, J. Dalibard, and S. Nascimbne, Nature Phys. **8**, 267 (Apr. 2012)
[6] D. M. Weld, P. Medley, H. Miyake, D. Hucul, D. E. Pritchard, and W. Ketterle, Phys. Rev. Lett. **103**, 245301 (Dec. 2009)
[7] D. M. Weld, H. Miyake, P. Medley, D. E. Pritchard, and W. Ketterle, Phys. Rev. A **82**, 051603 (Nov. 2010)
[8] C. J. M. Mathy, D. A. Huse, and R. G. Hulet, Phys. Rev. A **86**, 023606 (Aug. 2012)
[9] M. Gullans, T. G. Tiecke, D. E. Chang, J. Feist, J. D. Thompson, J. I. Cirac, P. Zoller, and M. D. Lukin, Phys. Rev. Lett. **109**, 235309 (Dec. 2012)
[10] C. M. Aegerter, S. H. Lloyd, C. Ager, S. L. Lee, S. Romer, H. Keller, and E. M. Forgan, J. Phys.: Condens. Matter **10**, 7445 (Aug. 1998)
[11] T. M. Riseman, P. G. Kealey, E. M. Forgan, A. P. Mackenzie, L. M. Galvin, A. W. Tyler, S. L. Lee, C. Ager, D. M. Paul, C. M. Aegerter, R. Cubitt, Z. Q. Mao, T. Akima, and Y. Maeno, Nature **396**, 242 (Nov. 1998)
[12] V. Moshchalkov, R. Woerdenweber, and W. Lang, *Nanoscience and Engineering in Superconductivity* (Springer-Verlag, 2010)
[13] M. Baert, V. V. Metlushko, R. Jonckheere, V. V. Moshchalkov, and Y. Bruynseraede, Phys. Rev. Lett. **74**, 3269 (Apr. 1995)
[14] V. V. Moshchalkov, M. Baert, V. V. Metlushko, E. Rosseel, M. J. Van Bael, K. Temst, R. Jonckheere, and Y. Bruynseraede, Phys. Rev. B **54**, 7385 (Sep. 1996)
[15] E. Rosseel, M. Van Bael, M. Baert, R. Jonckheere, V. V. Moshchalkov, and Y. Bruynseraede, Phys. Rev. B **53**, R2983(R) (Feb. 1996)
[16] D. J. Morgan and J. B. Ketterson, Phys. Rev. Lett. **80**, 3614 (Apr. 1998)
[17] A. N. Grigorenko, G. D. Howells, S. J. Bending, J. Bekaert, M. J. Van Bael, L. Van Look, V. V. Moshchalkov, Y. Bruynseraede, G. Borghs, I. I. Kaya, and R. A. Stradling, Phys. Rev. B **63**, 052504 (Jan. 2001)

[18] A. N. Grigorenko, S. J. Bending, M. J. Van Bael, M. Lange, V. V. Moshchalkov, H. Fangohr, and P. A. J. de Groot, Phys. Rev. Lett. **90**, 237001 (Jun. 2003)
[19] G. R. Berdiyorov, M. V. Milošević, and F. M. Peeters, Phys. Rev. B **74**, 174512 (Nov. 2006)
[20] C. Reichhardt and C. J. O. Reichhardt, Phys. Rev. B **76**, 064523 (Aug. 2007)
[21] R. Cao, L. Horng, T. C. Wu, J. C. Wu, and T. J. Yang, J. Phys.: Condens. Matt. **21**, 075705 (Feb. 2009), ISSN 0953-8984, 1361-648X
[22] M. L. Latimer, G. R. Berdiyorov, Z. L. Xiao, W. K. Kwok, and F. M. Peeters, Phys. Rev. B **85**, 012505 (Jan. 2012)
[23] Q. Chen, S. C. Bae, and S. Granick, Nature **469**, 381 (Jan. 2011)
[24] F. Romano and F. Sciortino, Nature Materials **10**, 171 (Mar. 2011)
[25] X. Mao, Q. Chen, and S. Granick, Nature Materials **12**, 217 (Mar. 2013)
[26] M. E. Cates, Nature Materials **12**, 179 (Feb. 2013)
[27] E. Babaev and M. Speight, Phys. Rev. B **72**, 180502 (Nov. 2005)
[28] M. Silaev and E. Babaev, Phys. Rev. B **84**, 094515 (Sep. 2011)
[29] M. Silaev and E. Babaev, Phys. Rev. B **85**, 134514 (Apr. 2012)
[30] J. Garaud, D. F. Agterberg, and E. Babaev, Phys. Rev. B **86**, 060513 (Aug. 2012)
[31] V. Moshchalkov, M. Menghini, T. Nishio, Q. H. Chen, A. V. Silhanek, V. H. Dao, L. F. Chibotaru, N. D. Zhigadlo, and J. Karpinski, Phys. Rev. Lett. **102**, 117001 (Mar. 2009)
[32] J. Gutierrez, B. Raes, A. V. Silhanek, L. J. Li, N. D. Zhigadlo, J. Karpinski, J. Tempere, and V. V. Moshchalkov, Phys. Rev. B **85**, 094511 (Mar. 2012)
[33] V. H. Dao, L. F. Chibotaru, T. Nishio, and V. V. Moshchalkov, Phys. Rev. B **83**, 020503 (Jan. 2011)
[34] C. W. Hicks, J. R. Kirtley, T. M. Lippman, N. C. Koshnick, M. E. Huber, Y. Maeno, W. M. Yuhasz, M. B. Maple, and K. A. Moler, Phys. Rev. B **81**, 214501 (Jun. 2010)
[35] S. J. Ray, A. S. Gibbs, S. J. Bending, P. J. Curran, E. Babaev, C. Baines, A. P. Mackenzie, and S. L. Lee, Phys. Rev. B **89**, 094504 (Mar. 2014)
[36] J. Carlström, E. Babaev, and M. Speight, Phys. Rev. B **83**, 174509 (May 2011)
[37] C. N. Varney, K. A. H. Sellin, Q.-Z. Wang, H. Fangohr, and E. Babaev, J. Phys.: Condens. Matter **25**, 415702 (Oct. 2013)
[38] L. Komendová, M. V. Milošević, and F. M. Peeters, Phys. Rev. B **88**, 094515 (Sep. 2013)
[39] H. Fangohr, A. R. Price, S. J. Cox, P. A. J. de Groot, G. J. Daniell, and K. S. Thomas, J. Comp. Phys. **162**, 372 (Aug. 2000)
[40] H. Fangohr, S. J. Cox, and P. A. J. de Groot, Phys. Rev. B **64**, 064505 (Jul. 2001)
[41] X. B. Xu, H. Fangohr, X. N. Xu, M. Gu, Z. H. Wang, S. M. Ji, S. Y. Ding, D. Q. Shi, and S. X. Dou, Phys. Rev. Lett. **101**, 147002 (Sep. 2008)
[42] J. A. Drocco, C. J. O. Reichhardt, C. Reichhardt, and A. R. Bishop, J. Phys.: Condens. Matter **25**, 345703 (Aug. 2013)
[43] G. Malescio and G. Pellicane, Phys. Rev. E **70**, 021202 (Aug. 2004)
[44] M. A. Glaser, G. M. Grason, R. D. Kamien, A. Komrlj, C. D. Santangelo, and P. Ziherl, Europhys. Lett. **78**, 46004 (May 2007)
[45] J. Pearl, Appl. Phys. Lett. **5**, 65 (1964)
[46] The definition of the density is: $\rho = N_v/L_xL_y$, where N_v is the number of vortices, L_x and L_y are the box size of simulation.
[47] The functional form of the potentials in Fig. 2 can be found in Appendix B of Ref. 37 (see Eq. (B.5)). The precise form of the potential is not particularly important as the two-dimensional lattices can be generated using a multitude of parameters, which we shall discuss elsewhere. The parameters for solid red line are $\alpha = 3.0$, $\beta = 1.5$, and $\xi = \lambda$ while for the dashed blue line are $\alpha = 2.5$, $\beta = 0.5$, and $\xi = \lambda$. In both cases, we set $c_1 = 1$, $c_2 = 0.2$, $c_3 = 0.1$, $\lambda = 1$, and $\delta = 0.1$.
[48] Q. Meng, C. N. Varney, H. Fangohr, and E. Babaev, (unpublished)